

Mechanically robust and stretchable silk/hyaluronic acid hydrogels

Burak Tavsanlı, Oguz Okay*

Department of Chemistry, Istanbul Technical University, 34469 Maslak, Istanbul, Turkey



ARTICLE INFO

Keywords:

Hyaluronic acid
Silk fibroin
Gelation
Hydrogels
Mechanical properties

ABSTRACT

Combining the material and biological properties of hyaluronic acid (HA) and silk fibroin (SF) in a single hydrogel would expand the range of applications available to HA and SF individually. Here, we present a novel strategy to prepare mechanically robust and stretchable SF/HA hydrogels. The hydrogels were prepared from methacrylated HA (MeHA) and SF in aqueous solutions in the presence of a radical initiator. N, N-dimethylacrylamide (DMAA) monomer was also included into the reaction solution as a spacer to connect MeHA's through their pendant vinyl groups. The presence of SF significantly enhances the mechanical strength of HA hydrogels due to its β -sheet domains acting as physical cross-links. The damage in SF network under large strain leads to a significant energy dissipation, which is responsible for the improved mechanical properties of SF/HA hydrogels.

1. Introduction

Hydrogels derived from natural polymers such as silk or hyaluronic acid have been used in a wide range of biological and biomedical applications because of their advantages including good biocompatibility and controlled degradability (Burdick & Prestwich, 2011; Hardy, Römer, & Scheibel, 2008; Highley, Prestwich, & Burdick, 2016; Kim, Park, Kim, H., & Kaplan, 2005; Lapčák, Lapčák, De Smedt, Demeester, & Chabreček, 1998; Melke, Midha, Ghosh, Ito, & Hofmann, 2016). Silk consists mainly of two components, namely fibroin and sericin proteins which are produced in the glands of domesticated silkworm *Bombyx mori* (Iizuka, 1969; Sasaki & Noda, 1974). Silk fibroin (SF) has a microstructure similar to multiblock copolymers composed of hydrophobic and hydrophilic blocks inside, together with hydrophilic terminal blocks (Jin & Kaplan, 2003; Zhou, 2000). The less ordered hydrophilic blocks of SF provide water solubility, elasticity and toughness whereas large hydrophobic blocks form intermolecular associations leading to a conformational transition from random-coil or helix to β -sheet structure. The β -sheets in silk fibroin acting as physical cross-links by connecting the fibroin molecules into a 3D network are responsible for the high strength of fibroin hydrogels.

Hyaluronic acid (HA) is a naturally occurring polyanion composed of disaccharide repeating units of β -1,4-D-glucuronic acid - β -1,3-N-acetyl-D-glucosamine (Fraser, Laurent, & Laurent, 1997). HA has unique lubricating properties and biological functions and hence, plays important roles in cell differentiation, cell motility, and wound-healing processes (Chen & Abatangelo, 1999; Zamboni, Viera, Reis, Oliveira, & Collins, 2018). Although HA is an important biomaterial for soft tissue

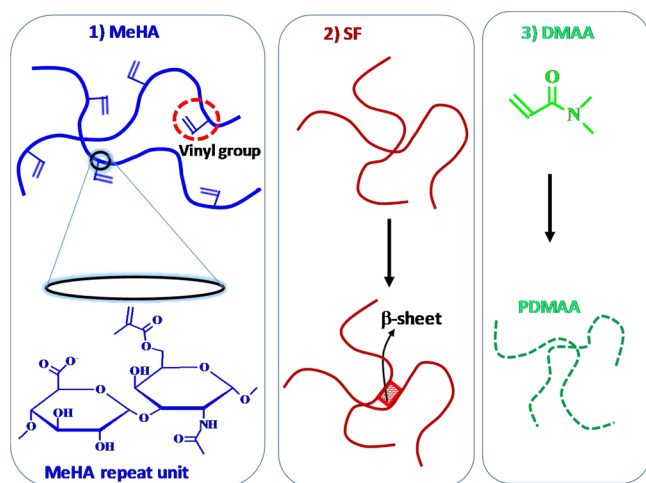
regeneration, poor biomechanical performance and rapid degradation of HA limit its applications (Collins & Birkinshaw, 2008; Valachova et al., 2016). To produce slowly degradable HA, it was physically or chemically cross-linked or, alternatively, methacrylate groups are incorporated into HA to generate HA macromers, which are then polymerized to form hydrogels (Leach, Bivens, Patrick, & Schmidt, 2003; Prado, Weaver, & Love, 2011; Tavsanlı, Can, & Okay, 2015).

Our aim in this study was to combine the material and biological properties of SF and HA in a single composite hydrogel that would expand the range of properties and hence applications available to SF and HA individually. The ionic nature of the HA component in such composites will provide enhanced water retention and structural support, whereas relative slow degradation and mechanical strength of SF component will contribute to the mechanical integrity and control of water interactions of HA. SF/HA scaffolds, hydrogels, patches, and films have been prepared in the past years using several techniques including ultrasonication (Hu et al., 2010; Park et al., 2011), cross-linking using enzymes (Raia et al., 2017), or chemical cross-linking agents such as genipin and carbodimides (Chi et al., 2012; Ren, Zhou, Liu, Xu, & Cui, 2009; Yan et al., 2018; Yang et al., 2016). The resulting composites exhibit, however, poor mechanical properties and have no stretchability limiting their applications. More recently, Zhou et al. (2016) prepared SF/HA films without a cross-linker or any post treatment capable of sustaining up to around 140% stretches. It was shown that the presence of HA enhances β -sheet formation in SF, which well correlates with improved mechanical properties of SF/HA films or hydrogels (Garcia-Fuentes, Giger, Meinel, & Merkle, 2008).

We describe here a novel strategy for the preparation of

* Corresponding author.

E-mail address: okayo@itu.edu.tr (O. Okay).



Scheme 1. Components of composite hydrogels. 1) methacrylated hyaluronic acid (MeHA), 2) silk fibroin (SF), and 3) in-situ formed PDMAA.

mechanically robust SF/HA hydrogels exhibiting a high stretchability up to around 400%. Instead of HA, methacrylated HA (MeHA) prepared by the reaction of HA with glycidyl methacrylate was used in the gel preparation (Scheme 1). Previous work shows that the hydrogels derived from MeHA show good biocompatibility and reduced degradation rate as compared to the native HA (Ibrahim, Kothapalli, Kang, & Ramamurthi, 2011; Leach et al., 2003; Weng, Gouldstone, Wu, & Chen, 2008). MeHA of various methacrylation degrees between 4 and 25% and SF isolated from *Bombyx mori* cocoons are the starting materials of the present composite hydrogels (Scheme 1). Due to the presence of pendant vinyl groups on MeHA molecules, they act both as a macromer and multifunctional chemical cross-linker during the radical polymerization in aqueous solutions (Tavsanlı & Okay, 2017). By conducting polymerization of MeHA in the presence of SF at an elevated temperature, we intend to induce β -sheet domains between SF molecules and hence, to produce additional cross-links of physical nature (Scheme 1). Preliminary experiments, however, showed no gel formation in aqueous solutions of MeHA and SF, likely because of the steric effect of SF hindering the cross-linking reactions between MeHA. Therefore, N, N-dimethylacrylamide (DMAA) monomer was also included into the reaction system as a spacer to connect MeHA's through their pendant vinyl groups. The in situ formed poly(DMAA) (PDMAA) is known to exhibit both associative and enhanced proton acceptor properties, which would contribute to the cooperativity of the non-covalent bonds in the composite hydrogels (Relógio, Martinho, & Farinha, 2005; Uemura, McNulty, & Macdonald, 1995). As will be seen below, the presence of SF significantly enhances the mechanical strength and toughness of MeHA hydrogels by creating an energy dissipation mechanism under load. Further, a wide range of tunable mechanical and swelling properties could be achieved by varying the methacrylation degree of MeHA. Because the hydrogel components MeHA, SF, and PDMAA exhibit good biocompatibility, the composite hydrogels presented here are a good candidate as biomaterials in biological and biomedical applications.

2. Experimental section

2.1. Materials

Hyaluronic acid sodium salt (HA, Sigma-Aldrich) from *Streptococcus equi* having a viscosity average molar mass of 1.2×10^6 g mol⁻¹ was used as received (Ström, Larsson, & Okay, 2015). Silk fibroin (SF) protein was separated from *Bombyx mori* cocoons (Koza Birlık, Bursa, Turkey), as reported earlier (Kim et al., 2004). Briefly, the cocoons were placed in boiling aqueous 0.02 M Na₂CO₃ solution for 1 h

for the removal of sericin protein. After thorough rinsing, the remaining fibroin was dissolved in 9.3 M LiBr aqueous solution at 60 °C and then the solution was dialyzed in a dialysis tube (10000 MWCO, Snake Skin, Pierce) against deionized water for 3 days. This procedure yielded an aqueous 5 wt. % SF solution. N,N-dimethylacrylamide (DMA, Sigma-Aldrich, 99%), glycidyl methacrylate (GM, Sigma Aldrich, 97%), tetrabutylammonium bromide (TBAB, Sigma-Aldrich, $\geq 99\%$), triethylamine (TEA, Merck, 99%), ammonium persulfate (APS, Sigma-Aldrich, $\geq 99\%$), N,N,N',N'-tetramethylethylenediamine (TEMED, Sigma-Aldrich, $\geq 99\%$), LiBr (Merck), and Na₂CO₃ (Merck) were used as received.

2.2. Methacrylation of HA

HA was methacrylated according to a procedure described previously (Leach et al., 2003). Briefly, 0.5 g of HA was dissolved in 50 mL distilled water and stirred overnight at 23 ± 2 °C. To prepare a solution containing 6-fold molar excess of GM with respect to the disaccharide repeat unit of HA, 1 mL of GM, 1 mL of TEA and 1 g of TBAB were added to the HA solution. After heating the solution to 55 °C and stirring for 1 h, it was cooled to 23 ± 2 °C and precipitated twice in a large excess of acetone. After dissolving the precipitate in water, the solution of methacrylated HA (MeHA) was freeze-dried (Christ Alpha 2e4 LD-plus) for 2 days. The degree of methacrylation (DM) of MeHA was determined by nuclear magnetic resonance using a 500 MHz Agilent VNMR spectrometer, as detailed before (Tavsanlı et al., 2015).

2.3. Preparation of composite hydrogels

The initial concentrations of DMAA, and SF were fixed at 5, and 2.5 w/v %, respectively, while MeHA was used at 1 and 2 w/v % concentrations at methacrylation degrees (DM) of 4, 14, and 25%. Typically, MeHA (0.100 or 0.200 g) was first dissolved overnight in 4.38 mL of water under gently stirring. After addition of DMAA monomer (0.500 g) and stirring for 30 min, 5 mL of a 5 w/v % SF solution were dropwise, slowly added to this solution with a rate of 1 mL min⁻¹ to prevent aggregations during fast mixing of the solutions (Hu et al., 2010). After bubbling nitrogen for 10 min and cooling to 4 °C, TEMED (25 μ L) and 0.1 mL of APS stock solution (0.08 g mL⁻¹) were added. The solution was then transferred into 1-mL plastic syringes and the reactions were conducted at 50 °C for 2 days. For 1 and 2 w/v % MeHA in the synthesis feed, the total solid contents of the hydrogels after preparation (C_0) were 8.9 and 10.0 w/v %, whereas MeHA:SF weight ratios were 1:2.5 and 1:1.25, respectively.

2.4. Rheological measurements

A Gemini 150 rheometer system (Bohlin Instruments) in the cone-and-plate mode (cone angle = 4°, diameter = 40 mm) equipped with a Peltier device for temperature control was used to measure the storage G' and loss moduli G'' as functions of the reaction time and angular frequency ω . To prevent evaporation of water, a solvent trap was used during the rheological measurements. The strain amplitude γ_0 in the measurements was fixed at 1% which was within the linear viscoelastic range of the hydrogels.

2.5. Swelling tests

The gel specimens were placed in an excess of water at 23 ± 2 °C for 4–7 days, replacing the water every other day. After reaching swelling equilibrium, the relative weight swelling ratio m_{rel} of the hydrogels was calculated as $m_{rel} = m/m_0$, where m and m_0 are the masses of the gel specimen in equilibrium swollen and as-prepared states, respectively. To determine the dry mass of the specimens, they were placed in acetone for 1 day which is a poor solvent for the polymers. After drying at 80 °C under vacuum to constant mass m_{dry} , the gel

fraction W_g , that is, the fraction of the total mass of MeHA, SF, and DMAA incorporated into the 3D polymer network was calculated as $W_g = m_{dry} / (m_o C_o)$.

2.6. XRD, DSC, and ATR-FTIR measurements

X-ray diffraction (XRD) patterns of freeze-dried samples were recorded in reflection mode on a PANalytical X-Pert PRO X-ray generator using Ni-filtered Cu K α ($\lambda = 0.15418$ nm) irradiation (45 kV, 40 mA) in the range of $2\theta = 5\text{--}40^\circ$. Differential scanning calorimetry (DSC) measurements were carried out on a Perkin Elmer Diamond DSC under nitrogen atmosphere. The freeze-dried polymer specimens sealed in aluminum pans were scanned between 30 and 300 °C with heating and cooling rates of 10 °C min $^{-1}$. Fourier transform infrared (FTIR) spectra of the polymers were recorded on a Nicolet Nexus 6700 spectrophotometer using a single-bounce diamond attenuated total reflectance (ATR) accessory equipped with a liquid nitrogen cooled mercury–cadmium–telluride (MCT) detector. 64 interferograms at 4 cm $^{-1}$ resolution were co-added to generate each spectrum.

2.7. Mechanical tests

Uniaxial compression and tensile tests were carried out at 23 ± 2 °C with a Zwick Roell test machine, model Z0.5 TH, using a 500 N load cell. For the compression tests, cubic gel specimens with dimensions $3 \times 3 \times 3$ mm were prepared by cutting as-prepared and swollen hydrogels. To ensure a complete contact between the specimen and the plates, an initial compressive force of 0.01 N was applied before the test. The tests were conducted at a strain rate of 0.3 and 1 mm min $^{-1}$ below and above 15% compression, respectively. Nominal σ_{nom} and true σ_{true} stresses ($\sigma_{true} = \lambda \sigma_{nom}$) were used in the calculations, which are the forces acting per unit area of the undeformed and deformed gel specimens, respectively, and λ is the deformation ratio. The strain is given by fractional deformation ϵ which is equal to $1 - \lambda$ or $\lambda - 1$, for compression and elongation, respectively. Compressive fracture stress σ_f was calculated from the maxima of σ_{true} vs ϵ curves, as detailed previously (Argun, Can, Altun, & Okay, 2014). Young's modulus E was calculated from the slope of the stress-strain curves between 5 and 15% deformations. Cyclic compression tests were carried out by compressing the gel specimens at a strain rate of 1 mm min $^{-1}$ up to a predetermined maximum strain, and then unloading with the same strain rate to zero strain. These loading and unloading steps were repeated with a wait time of 1 min between the cycles. Uniaxial tensile tests were conducted using cylindrical gel specimens of 4.6 mm in diameter and 10 ± 2 mm in length at a strain rate of 5 mm min $^{-1}$.

3. Results and discussion

Methacrylated hyaluronic acid (MeHA), silk fibroin (SF), and N, N'-dimethyl acrylamide (DMAA) are the starting materials of the present biocompatible, biodegradable composite hydrogels (Scheme 1). The

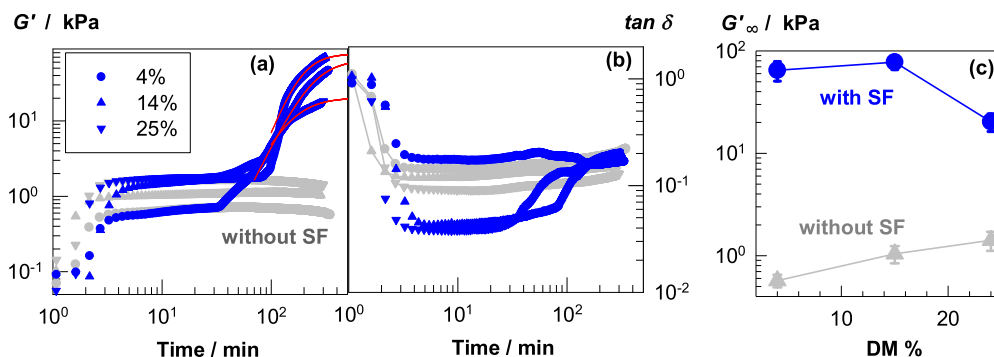


Fig. 1. (a, b): Storage modulus G' (a) and the loss factor $\tan \delta$ (b) of the reaction solutions plotted against the reaction time. $\omega = 6.3$ rad s $^{-1}$. $\gamma_o = 0.01$. Temperature = 50 °C. MeHA = 1 w/v%. Methacrylation degrees (DM) of MeHA are indicated. Gray symbols represent the data obtained in the absence of silk fibroin. (c): Limiting modulus (G'_∞) of the hydrogels with and without SF plotted against DM.

methacrylation degree of MeHA was determined as 4, 14, and 25% for the molar ratios of glycidyl methacrylate to disaccharide repeat units of 6, 24, and 49, respectively. The initial concentrations of DMAA, and SF were fixed at 5.0, and 2.5 w/v %, respectively, while MeHA was used at 1 and 2 w/v % concentrations with methacrylation degrees (DM) of 4, 14, and 25%. To highlight the effect of SF, all gelation reactions were also conducted in the absence of SF. In the following paragraphs, we first discuss gelation mechanism of the reaction system and then describe the viscoelastic, swelling, and mechanical properties of the hydrogels by highlighting significant effects of SF and methacrylation degree of HA on the hydrogel properties.

3.1. Gelation

We monitored hydrogel formation by rheometry using oscillatory deformation tests at an angular frequency ω of 6.3 rad s $^{-1}$ and strain amplitude γ_o of 1%. Blue symbols in Fig. 1a and b show the storage modulus G' and the loss factor $\tan \delta$ ($= G''/G'$ where G'' is the loss modulus) of the reaction solutions, respectively, plotted against the reaction time. MeHA macromers with three different degrees of methacrylation (DM) were used in the gel preparation, as indicated in the figure. During the initial period of the reaction, G' rapidly increases to around 1 kPa and $\tan \delta$ decreases to around 0.1 followed by a plateau regime where G' and $\tan \delta$ remain almost unchanged. However, at longer times, G' starts to increase again and approaches a second plateau at 10^2 kPa. We have to note that, to prevent evaporation of water, the reactions between the plates of the rheometer could be monitored up to 5 h (Fig. 1a). Therefore, the limiting moduli G'_∞ of the hydrogels was estimated by fitting the data of the second reaction period to the modified Hill equation (Calvet, Wong, & Giasson, 2004; Giraldo, Vivas, Vila, & Badia, 2002; Tavsanlı & Okay, 2016)

$$G'(t) = G'_\infty \frac{t^n}{t^n + \theta^n} \quad (1)$$

where θ and n are constants. The solid red curves in Fig. 1a are the best fits of Eq. (1) to the experimental data yielding G'_∞ as 65, 78, and 20 kPa at 4, 14, and 25% DM, respectively (Fig. 1c).

To explain this unusual two-step gelation profile of the reaction system, we repeated the measurements on the same reaction solutions but without including silk fibroin (SF). The results are also shown in Fig. 1a and b by gray triangles. It is seen that, in the absence of SF, the first reaction period closely matches to that with SF whereas the second period disappears from the gelation profile, suggesting that the second rise in G' is due to the presence of SF in the reaction system. The final modulus of the hydrogels without SF shown in Fig. 1c by the gray symbols is more than one-order of magnitude smaller than that with SF. The results indicate that the cross-linking copolymerization of MeHA and DMAA during the first reaction period dominates the viscoelastic properties of the reaction system and produces hydrogels with a modulus of around 1 kPa, whereas at longer times fibroin gelation dominates their viscoelasticity by further increasing the modulus to 20–78 kPa.

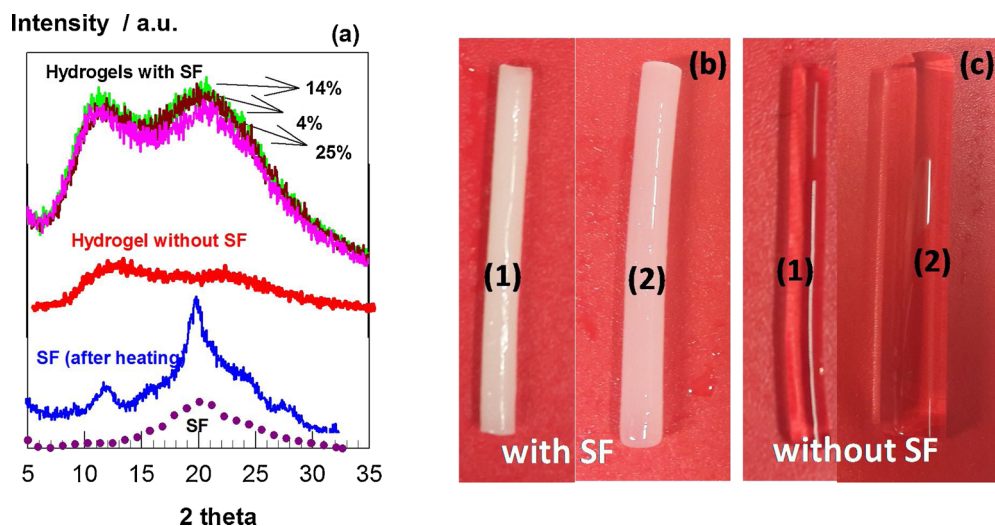


Fig. 2. (a): X-ray diffraction of freeze-dried 2.5 w/v % SF solutions before (dotted curve) and after heating to 50 °C (blue curve), and composite hydrogels with and without SF. Methacrylation degree DM of MeHA is indicated. (b, c): Photographs of the hydrogels with (b) and without SF in as-prepared (1) and swollen states in water (2). (For interpretation of the references to colour in this figure legend, the reader is referred to the web version of this article).

Previous work shows that gelation of aqueous SF solutions occurs due to the conformational transition in SF from random-coil or helix to β -sheet structures leading to the formation of SF hydrogels in which intermolecular β -sheets act as physical cross-links (Vepari & Kaplan, 2007; Vollrath & Porter, 2009). Because the rate of fibroin gelation is slow as compared to many proteins gels, one may expect that β -sheet structures start to form in the present reaction system during the second period of the reaction accompanied with a significant increase in the modulus G' . FTIR technique is a mean to detect conformational transitions in silk fibroin and to estimate the β -sheet contents. Amide I region of the FTIR spectrum of SF is characterized by a broad peak at around 1640 cm^{-1} due to the presence of primarily random-coil and α -helix conformations while appearance of a main peak at 1620 cm^{-1} indicates β -sheet conformation (Fig. S1) (Chen, Knight, Shao, & Vollrath, 2002; Karakutuk, Ak, & Okay, 2012). However, PDMAA component of the hydrogel also exhibited a peak at 1610 cm^{-1} due to C=O stretching and hence, this technique could not be used to estimate the content of the β -sheets in the hydrogels (Fig. S1).

Therefore, the structure of SF in the hydrogels was assessed by XRD measurements. Fig. 2a shows typical X-ray profiles of freeze-dried hydrogels with and without SF together with SF alone. SF exhibits a broad peak from 15 to 28° indicating an amorphous structure (dotted curve) (Kim et al., 2004). To induce β -sheet domains in SF, an aqueous solution of 2.5 w/v% SF was heated at 50 °C for 2 h. The blue curve in Fig. 2b represents XRD pattern of this SF solution after freeze-drying. It exhibits diffraction peaks at 2θ values of 11°, 20.5°, and a shoulder at 24° corresponding to crystalline spacings of 0.80, 0.43, and 0.37 nm, which are typical for Silk II structure (Ayub, Arai, & Hirabayashi, 1993; Kim et al., 2004). Thus, as expected, a conformational transition from random-coil and helix to the β -sheet structure occurs after heating SF solution to 50 °C. Fig. 2a also shows that freeze dried hydrogels exhibit the same peaks while no distinct peaks appear in the XRD pattern of SF-free hydrogel. Thus, XRD results confirm the formation of β -sheet structure during the gelation reactions leading to a significant increase in the modulus of the hydrogels.

Formation of nano-sized crystalline domains in the hydrogels was also reflected from their visual appearances. Fig. 2b and c show images of the hydrogels prepared with and without silk fibroin, respectively, in as-prepared (1) and equilibrium swollen states in water (2). As compared to the transparent SF-free hydrogels, those containing SF are opaque and exhibit a lesser degree of swelling reflecting the effect of β -sheets as additional cross-links. DSC measurements conducted on freeze-dried hydrogels showed a broad endothermic peak at around 100 °C due to the loss of moisture remaining after freeze-drying (Fig. S2). However, the characteristic peaks of the gel components SF, MeHA,

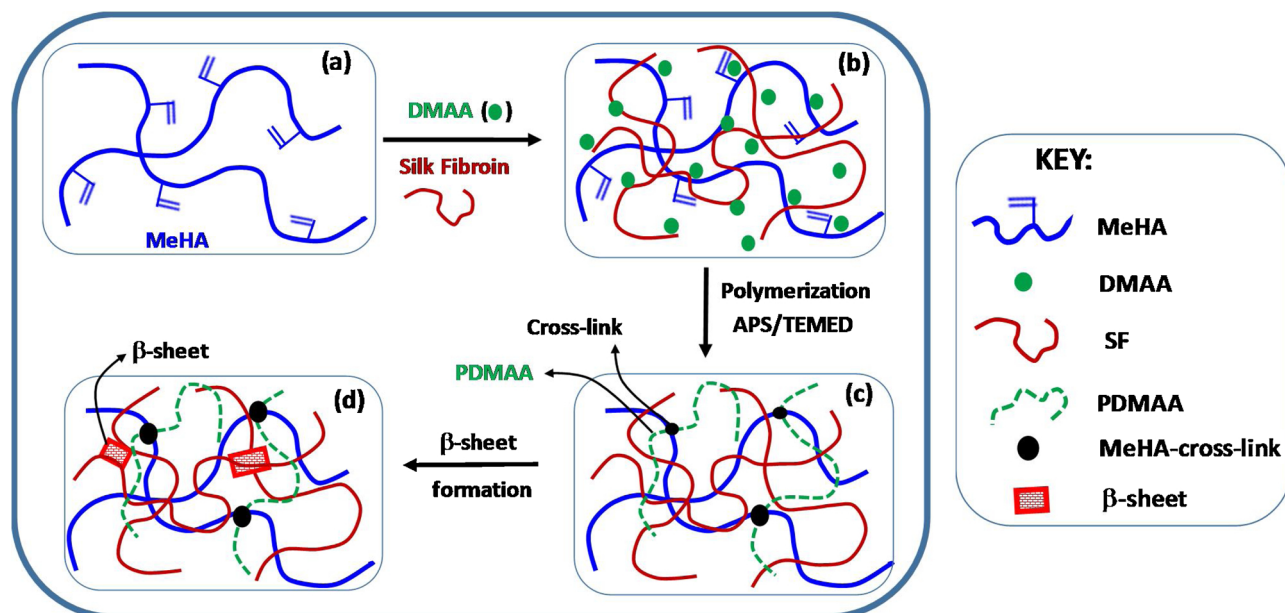
and PDMAA did not appear in the DSC scans of the hydrogels, and they all start to degrade at around 300 °C (Fig. S2).

The following scenario may explain the two-step gelation mechanism of the present system (Scheme 2). After addition of APS/TEMED redox initiator system into the reaction solution containing MeHA, DMAA and SF, primary radicals attack to DMAA monomer to produce growing PDMAA chains interconnected by MeHA cross-links (Scheme 2a–c). These reactions result in MeHA-cross-linked hydrogels with a storage modulus of around 1 kPa (Scheme 2c). Because of the slow rate of fibroin gelation, conformational transition in fibroin starts at longer reaction times leading to a second rise in the storage modulus due to the increasing number of β -sheets acting as additional cross-links (Scheme 2d).

3.2. Hydrogel properties

Composite hydrogels after a reaction time of 5 h were subjected to frequency-sweep tests at 25 °C and at a strain amplitude γ_0 of 1%. Fig. 3 shows the storage G' (filled symbols) and loss moduli G'' (open symbols) of the hydrogels prepared with and without SF plotted against the angular frequency ω . The methacrylation degree of MeHA is 4 (a), 14 (b), and 25% (c). The hydrogels prepared without SF exhibit typical behavior of HA hydrogels (Tavsanlı & Okay, 2016), i.e., at low ω , G'' attains low values and $\tan \delta$ approaches to 0.01 (not shown in the figures), corresponding elastic, solid-like behavior. At high ω , G'' approaches to G' and the gels exhibit a viscous character. After incorporation of fibroin into the hydrogel network, both moduli become slightly frequency dependent and no crossover of G' and G'' occurs. Further, G' modulus becomes one-order of magnitude higher than that of SF-free gels highlighting significant effect of fibroin on the hydrogel properties. The results also show that G' first increases with increasing DM from 4 to 14% but then decreases with a further increase in DM to 25%. The decrease of the modulus at 25% DM is also observable in the gelation profiles (Fig. 1) which is attributed to the steric effect of chemical MeHA-cross-links hindering formation of β -sheet domains.

After a reaction time of 2 days, hydrogels were subjected to the solubility and swelling tests in water. All hydrogels with or without SF were insoluble in water with a gel fraction between 0.85 and 0.98 indicating that MeHA, SF, and PDMAA components are incorporated into the 3D network (Table 1). Fig. 4a shows the degree of swelling (m_{rel}) of the hydrogels plotted against the methacrylation degree (DM) of MeHA. As expected from the storage moduli of the hydrogels (Fig. 1c), those with SF swell much less than without SF because of the presence of β -sheet cross-links. Further, the higher the DM, the lower is the degree of swelling of the hydrogels with or without SF, reflecting the effect of the



Scheme 2. Cartoon showing formation of silk-hyaluronic acid hydrogels using DMAA monomer acting as a spacer.

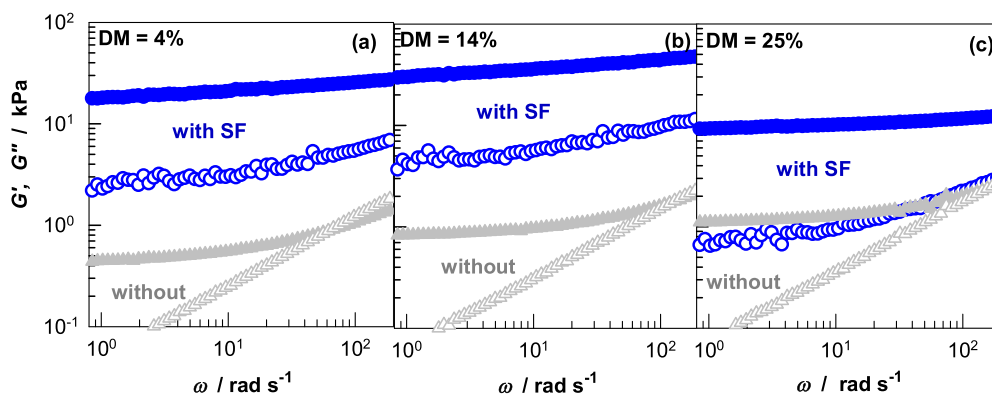


Fig. 3. G' (filled symbols), and G'' (open symbols) of the hydrogels with (blue circles) and without SF (gray triangles). $\gamma_o = 0.01$. MeHA = 1 w/v%. DM = 4 (a), 14 (b), and 25% (c). Temperature = 25 °C. (For interpretation of the references to colour in this figure legend, the reader is referred to the web version of this article).

Table 1

Compositions, swelling and compressive mechanical properties of the hydrogels. Standard deviations are shown in the parentheses. They are less than 5% for m_{rel} and W_g values. Note that for each hydrogel, at least five swelling and mechanical measurements from different specimens were averaged. (see Table S1 for the tensile mechanical properties).

DM %	MeHA w/v%	SF w/v%	m_{rel}	H ₂ O %	W_g	As-prepared state			After equilibrium swelling		
						σ_f / MPa	E / kPa	ϵ_f %	σ_f / kPa	E / kPa	ϵ_f %
4	1	2.5	2.8	98	0.92	4.9	54 (5)	94	448 (98)	14 (1)	78
14	1	2.5	2.2	98	0.95	3.4	82 (5)	91	323 (49)	41 (9)	70
25	1	2.5	1.9	99	0.96	2.5	99 (11)	86.6	288 (21)	48 (3)	70
4	2	2.5	4.7	97	0.87	3	30 (3)	85	224 (40)	42 (5)	63
14	2	2.5	3.1	97	0.89	1.1	52 (4)	77	207 (39)	59 (5)	59
25	2	2.5	2.2	98	0.85	0.9	81 (11)	70	118 (19)	99 (8)	48
4	1	0	17.2	98	0.96	0.6	5	88	85 (7)	4	72
14	1	0	9.3	96	0.97	0.4	8	84	51 (5)	5	62
25	1	0	5.3	98	0.97	0.4	13 (2)	79	26 (6)	11 (2)	53
4	2	0	13.6	99	0.96	1.2	11(1)	88	31 (3)	6	62
14	2	0	7.1	97	0.97	0.6	17 (3)	82	79 (3)	13 (1)	59
25	2	0	4.5	98	0.98	0.4	22 (3.3)	74	57 (4)	18 (1)	54

functionality of MeHA cross-linker on the gel cross-link density.

Mechanical properties of the hydrogels were determined by uniaxial compression and tensile tests. Figs. 5a and b show compressive stress-strain curves of the hydrogels prepared using MeHA with different degrees of methacrylation DM in their as-prepared (a) and swollen

states (b). The gray curves are the data obtained from hydrogels prepared without SF addition. A significant increase in both stiffness and fracture stress is observable upon incorporation of SF in the gel network. For instance, at DM = 4%, both Young's modulus E and fracture stress σ_f of as-prepared gels increase from 5 to 54 ± 5 kPa and from 0.6

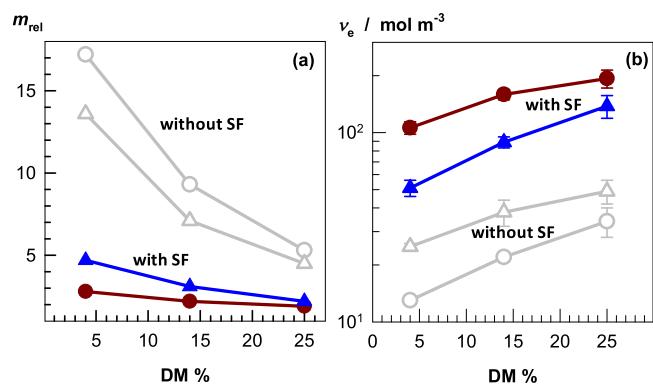


Fig. 4. Swelling ratio m_{rel} (a) and effective cross-link density ν_e of composite hydrogels plotted against the methacrylation degree (DM) of MeHA. Gray symbols represent data of the hydrogels without SF. MeHA = 1 (●, ○), and 2 w/v % (▲, △).

to 4.9 MPa, respectively, after incorporation of SF in the gel network (Fig. 6). Simultaneously, the toughness W calculated from the area under the stress-strain curves up to the fracture point increases from 19 ± 2 to $320 \pm 6 \text{ kJ m}^{-3}$ after SF addition (Table S2).

Moreover, increasing the methacrylation degree DM also increases the modulus E of the hydrogels whereas the fracture stress σ_f and strain ϵ_f decrease (Fig. 6). A similar effect was observed upon increasing MeHA content of the hydrogels (Fig. S3). Because increasing DM or MeHA concentration also increases the number of pendant vinyl groups in the reaction system, the chemical cross-link density and hence the modulus increases but the toughness decreases due to the stress localization in chemically cross-linked networks under stress (Creton, 2017). An opposite effect appears upon incorporation of SF indicating that fibroin molecules interconnected by the β -sheet domains reduces stress localization and creates energy dissipation mechanism in the gel network. The results also show that swelling of the hydrogels decreases their mechanical properties due to the dilution of the network chains. However, they still exhibit a high modulus (up to $99 \pm 8 \text{ kPa}$) in

equilibrium with water (Fig. 6). Uniaxial tensile tests could only be conducted on as-prepared hydrogels because they were too slippery after equilibrium swelling in water. Tensile stress-strain curves shown in Fig. 5c reveal that highly stretchable hydrogels were obtained at the lowest methacrylation degree DM of 4%. They sustain up to $350 \pm 50\%$ stretch ratio under a stress of $70 \pm 10 \text{ kPa}$ (Fig. 6f. See also Supporting Information Movie). Because silk fibroin hydrogels are usually brittle in tension, presence of MeHA seems to contribute to the stretchability of the composite hydrogels. Comparing tensile behavior of the hydrogels with and without SF reveals that stretch at break slightly reduces while tensile strength more than one order of magnitude increases after inclusion of SF in the gel network.

From the swelling ratios m_{rel} of the hydrogels in water together with their Young's moduli E , we estimated their effective cross-link densities ν_e using the theory of elasticity (Flory, 1953; Treloar, 1975),

$$E = 3 \nu_e R T (m_{rel})^{2/3} \quad (2)$$

where R is the gas constant and T is the absolute temperature. Eq. (2) assumes affine deformation of the polymer chains in the hydrogels under strain, and equality of the mass and volume swelling ratios. Fig. 4b shows the cross-link density ν_e of the hydrogels with (filled symbols) and without SF (open symbols) plotted against DM. Incorporation of SF into the gel network enhances its cross-link density, and the enhancement effect becomes stronger with increasing degree of methacrylation of MeHA. For instance, assuming additivity of the cross-links due to the MeHA cross-links and β -sheets, the contribution of β -sheets to the cross-link density increases from ~30 to 60–70% with increasing DM from 4 to 25%. Thus, composite hydrogels exhibit a hybrid cross-linked structure composed of chemical and physical cross-links.

For a deeper understanding of the nature of intermolecular bonds and the enhanced mechanical properties due to SF incorporation into the composite hydrogels, successive cyclic compression tests were conducted on the hydrogels prepared at DM = 4%. The tests consist of a loading step up to a maximum strain ϵ_{max} followed by the unloading step to zero strain. For an ideal elastic material, stress-strain curve of the unloading should follow that of the loading because there is no dissipation of the mechanical energy given to the material. Existence of

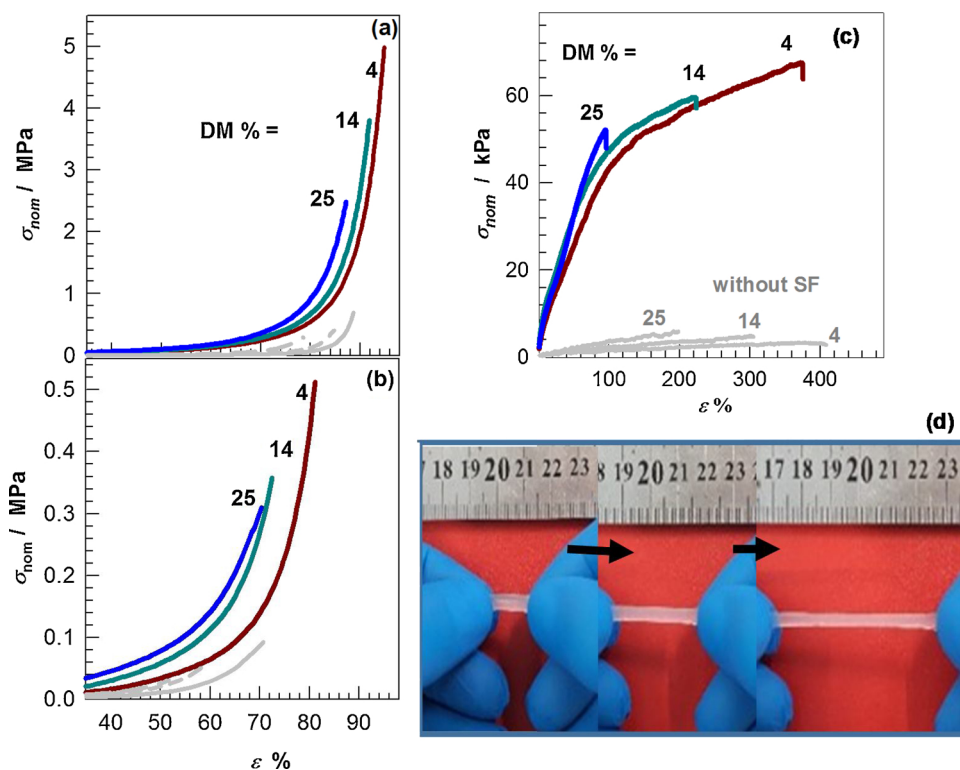


Fig. 5. (a, b): Compressive stress-strain curves of the hydrogels in as-prepared (a) and water-swollen states (b). MeHA = 1 w/v %. The data of SF-free hydrogels are shown by the gray solid, short-dash, and long-dash curves corresponding to DM = 4, 14, and 25%, respectively. (c): Tensile stress-strain curves of the hydrogels in as-prepared state. MeHA = 1 w/v %. (d): Photograph of a hydrogel sample with DM = 4% during stretching by hand to around 300% stretch ratio.

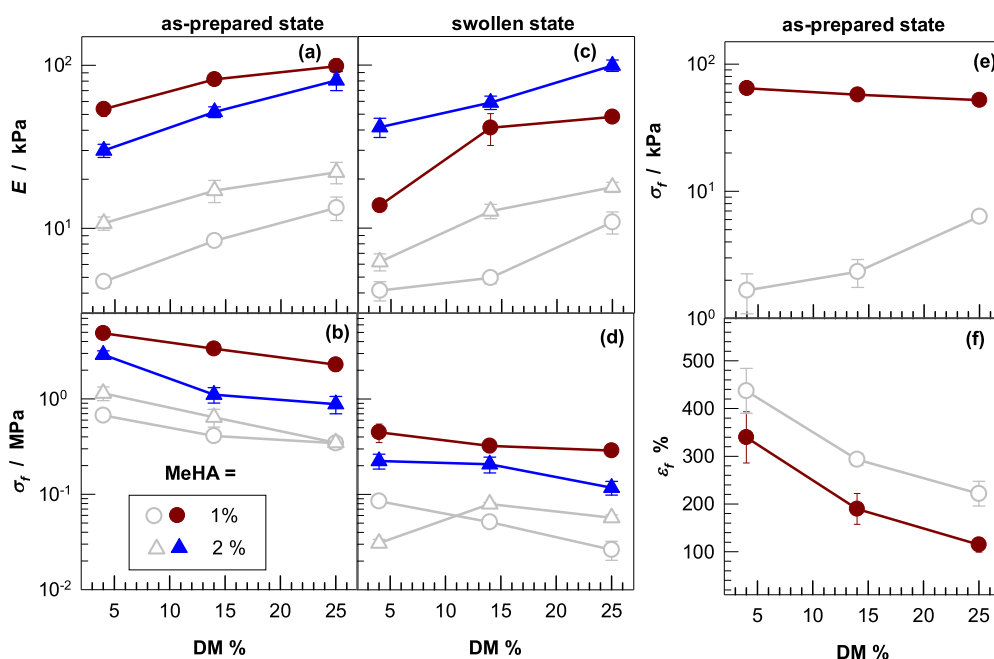


Fig. 6. (a–d): Young's modulus E and compressive strength σ_f of the hydrogels in as-prepared (left panel) and water-swollen states (right panel) plotted against the methacrylation degree (DM) of MeHA. Gray symbols represent the data of the hydrogels without SF. (e, f): Tensile strength σ_f and strain ϵ_f of the hydrogels with (filled symbols) and without SF (open symbols). MeHA = 1 w/v%.

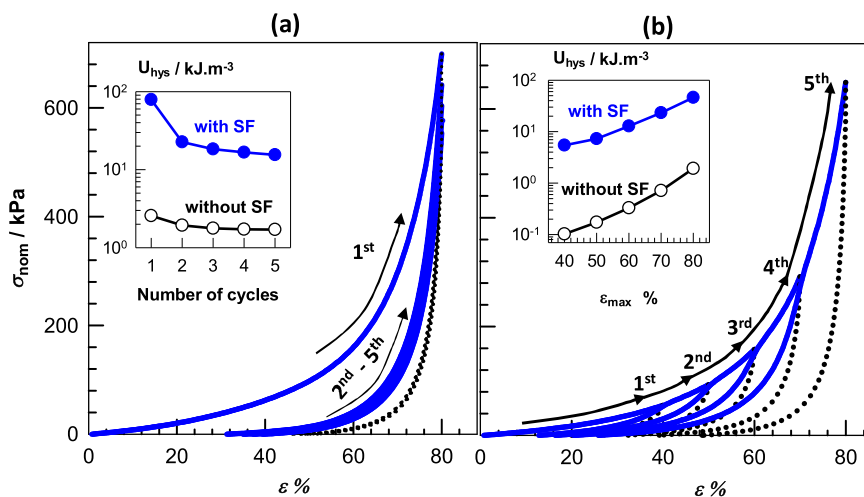


Fig. 7. Five successive compressive cyclic tests conducted up to a constant ϵ_{\max} of 80% (a) and with successively increasing ϵ_{\max} from 40 to 80% in five steps (b). Loading curves are indicated by the arrows. DM = 4%. MeHA = 1 w/v %. The insets show U_{hys} plotted against the number of cycles (a) and ϵ_{\max} (b).

energy dissipation under strain is reflected by the deviation between the paths of loading and unloading steps. Fig. 7a shows five successive compressive cycles up to $\epsilon_{\max} = 80\%$ while Fig. 7b shows the same cycles but with successively increasing ϵ_{\max} from 40 to 80% in five steps. The wait time between each cycle for the relaxation of the gel specimens was fixed at 1 min. For a fixed ϵ_{\max} of 80%, the first unloading strongly deviates from the loading indicating a significant energy dissipation due to the damage in the sample, i.e., due to the breaking of intermolecular bonds. However, the extent of this deviation decreases in the following cycles revealing that most of the bonds are broken during the first loading step.

The filled and open symbols in the insets to the figures represent the hysteresis energies U_{hys} of the hydrogels with and without SF, respectively, calculated from the area between loading and unloading curves. Note that the hysteresis energy U_{hys} is directly related to the total number of bonds broken during compression up to ϵ_{\max} (Creton, 2017; Uzumcu, Guney, & Okay, 2018). As compared to the SF-free hydrogel, a significant hysteresis appears in composite hydrogel revealing damage of a larger number of β -sheet cross-links of the SF component (Fig. 7a). The inset to Fig. 7b show that the dissipated energy U_{hys} also increases

with increasing maximum strain ϵ_{\max} , and the extent of U_{hys} increase is much larger in the composite hydrogels as compared to the SF-free ones. We attribute the enhancement in the mechanical properties of the hydrogels upon incorporation of SF to the energy dissipation of SF network under strain. For instance, the toughest hydrogel reported so far in the literature are double-network (DN) hydrogels composed of a brittle first network and ductile second network (Gong, Katsuyama, Kurokawa, & Osada, 2003). The first network in DN's breaks into smaller clusters under strain by dissipating energy whereas the second network keeps the macroscopic gel sample together, leading to extraordinary mechanical properties. For the present composite hydrogels, β -sheet domains of the brittle SF network break under strain by dissipating energy leading to improved mechanical properties as compared to the individual SF or HA hydrogels.

4. Conclusions

We presented a novel strategy for the preparation of mechanically robust and stretchable hydrogels composed of HA and SF components. Composite hydrogels were synthesized from methacrylated HA

(MeHA), SF, and DMAA in aqueous solutions in the presence of APS/TEMED redox initiator system. It was found that in-situ produced PDMAA chains are interconnected by MeHA cross-links whereas SF undergoes a conformation transition from random coil to β -sheet structures. A significant enhancement in the mechanical strength of the hydrogels was observed upon incorporation of SF due to its β -sheet domains acting as additional physical cross-links. Cyclic mechanical tests reveal that the damage in SF network under strain leads to a significant energy dissipation, which is responsible for the improved mechanical properties of SF/HA hydrogels. A wide range of tunable mechanical and swelling properties could be achieved by varying the methacrylation degree of MeHA. Because MeHA, SF, and PDMAA exhibit good biocompatibility, the composite hydrogels presented here are a good candidate as biomaterials in biological and biomedical applications. Moreover, because HA and SF components were combined in a single hydrogel material, present results would expand the range of properties and applications available to HA and SF individually.

Acknowledgements

The work was supported by Istanbul Technical University (ITU), BAP 39957. O. O. thanks Turkish Academy of Sciences (TUBA) for the partial support.

Appendix A. Supplementary data

Supplementary material related to this article can be found, in the online version, at doi:<https://doi.org/10.1016/j.carbpol.2018.12.088>.

References

- Argun, A., Can, V., Altun, U., & Okay, O. (2014). Nonionic double and triple network hydrogels of high mechanical strength. *Macromolecules*, *47*(18), 6430–6440.
- Ayub, Z. H., Arai, M., & Hirabayashi, K. (1993). Mechanism of the gelation of fibroin solution. *Bioscience Biotechnology and Biochemistry*, *57*(11), 1910–1912.
- Burdick, J. A., & Prestwich, G. D. (2011). Hyaluronic acid hydrogels for biomedical applications. *Advanced Materials*, *23*(12), 41–56.
- Calvet, D., Wong, J. Y., & Giasson, S. (2004). Rheological monitoring of polyacrylamide gelation: Importance of cross-link density and temperature. *Macromolecules*, *37*(20), 7762–7771.
- Chen, W. Y. J., & Abatangelo, G. (1999). Functions of hyaluronan in wound repair. *Wound Repair and Regeneration*, *7*(2), 79–89.
- Chen, X., Knight, D. P., Shao, Z., & Vollrath, F. (2002). Conformation transition in silk protein films monitored by time-resolved Fourier transform infrared spectroscopy: Effect of potassium ions on Nephila spidroin films. *Biochemistry*, *41*(50), 14944–14950.
- Chi, N. H., Yang, M. C., Chung, T. W., Chen, J. Y., Chou, N. K., & Wang, S. S. (2012). Cardiac repair achieved by bone marrow mesenchymal stem cells/silk fibroin/hyaluronic acid patches in a rat of myocardial infarction model. *Biomaterials*, *33*(22), 5541–5551.
- Collins, M. N., & Birkinshaw, C. (2008). Physical properties of crosslinked hyaluronic acid hydrogels. *Journal of Materials Science Materials in Medicine*, *2008*(19), 3335–3343.
- Creton, C. (2017). 50th Anniversary perspective: Networks and gels: Soft but dynamic and tough. *Macromolecules*, *50*, 8297–8316.
- Flory, P. J. (1953). *Principles of polymer chemistry*. Ithaca, NY: Cornell University Press.
- Fraser, J. R. E., Laurent, T. C., & Laurent, U. B. G. (1997). Hyaluronan: Its nature, distribution, functions and turnover. *Journal of Internal Medicine*, *242*(1), 27–33.
- Garcia-Fuentes, M., Giger, E., Meinel, L., & Merkle, H. P. (2008). The effect of hyaluronic acid on silk fibroin conformation. *Biomaterials*, *29*(6), 633–642.
- Giraldo, J., Vivas, N. M., Vila, E., & Badia, A. (2002). Assessing the (a)symmetry of concentration-effect curves: Empirical versus mechanistic models. *Pharmacology & Therapeutics*, *95*(1), 21–45.
- Gong, J. P., Katsuyama, Y., Kurokawa, T., & Osada, Y. (2003). Double-network hydrogels with extremely high mechanical strength. *Adv. Mater.*, *15*, 1155–1158.
- Hardy, J. G., Römer, L. M., & Scheibel, T. R. (2008). Polymeric materials based on silk proteins. *Polymer*, *49*(20), 4309–4327.
- Highley, C. B., Prestwich, G. D., & Burdick, J. A. (2016). Recent advances in hyaluronic acid hydrogels for biomedical applications. *Current Opinion in Biotechnology*, *40*, 35–40.
- Hu, X., Lu, Q., Sun, L., Cebe, P., Wang, X., Zhang, X., & Kaplan, D. L. (2010). Biomaterials from ultrasonication-induced silk fibroin-hyaluronic acid hydrogels. *Biomacromolecules*, *11*(11), 3178–3188.
- Ibrahim, S., Kothapalli, C. R., Kang, Q. K., & Ramamurthi, A. (2011). Characterization of glycidyl methacrylate – crosslinked hyaluronan hydrogel scaffolds incorporating elastogenic hyaluronan oligomers. *Acta Biomaterialia*, *7*(2), 653–665.
- Iizuka, E. (1969). Conformation of silk sericine in solution, Bombyx mori L. *Biochimica et Biophysica Acta (BBA) – Protein Structure*, *181*(2), 477–479.
- Jin, H.-J., & Kaplan, D. L. (2003). Mechanism of silk processing in insects and spiders. *Nature*, *424*(6952), 1057–1061.
- Karakutuk, I., Ak, F., & Okay, O. (2012). Diepoxide-triggered conformational transition of silk fibroin: Formation of hydrogels. *Biomacromolecules*, *13*(4), 1122–1128.
- Kim, U. J., Park, J., Joo Kim, H., Wada, M., & Kaplan, D. L. (2005). Three-dimensional aqueous-derived biomaterial scaffolds from silk fibroin. *Biomaterials*, *26*(15), 2775–2785.
- Kim, U. J., Park, J., Li, C., Jin, H. J., Valluzzi, R., & Kaplan, D. L. (2004). Structure and properties of silk hydrogels. *Biomacromolecules*, *5*(3), 786–792.
- Lapčák, L., Lapčák, L., De Smedt, S., Demeester, J., & Chabreček, P. (1998). Hyaluronan: Preparation, structure, properties, and applications. *Chemical Reviews*, *98*(8), 2663–2684.
- Leach, J. B., Bivens, K. A., Patrick, C. W., & Schmidt, C. E. (2003). Photocrosslinked hyaluronic acid hydrogels: Natural, biodegradable tissue engineering scaffolds. *Biotechnology and Bioengineering*, *82*(5), 578–589.
- Melke, J., Midha, S., Ghosh, S., Ito, K., & Hofmann, S. (2016). Silk fibroin as biomaterial for bone tissue engineering. *Acta Biomaterialia*, *31*, 1–16.
- Park, S.-H., Cho, H., Gil, E. S., Mandal, B. B., Min, B.-H., & Kaplan, D. L. (2011). Silk-Fibrin/Hyaluronic acid composite gels for nucleus pulposus tissue regeneration. *Tissue Engineering Part A*, *17*(23–24), 2999–3009.
- Prado, S. S., Weaver, J. M., & Love, B. J. (2011). Gelation of photopolymerized hyaluronic acid grafted with glycidyl methacrylate. *Materials Science and Engineering C*, *31*(8), 1767–1771.
- Raia, N. R., Partlow, B. P., McGill, M., Kimmerling, E. P., Ghezzi, C. E., & Kaplan, D. L. (2017). Enzymatically crosslinked silk-hyaluronic acid hydrogels. *Biomaterials*, *131*, 58–67.
- Relógio, P., Martinho, J. M. G., & Farinha, J. P. S. (2005). Effect of surfactant on the intra- and intermolecular association of hydrophobically modified poly(N,N-dimethylacrylamide). *Macromolecules*, *38*(26), 10799–10811.
- Ren, Y. J., Zhou, Z. Y., Liu, B. F., Xu, Q. Y., & Cui, F. Z. (2009). Preparation and characterization of fibroin/hyaluronic acid composite scaffold. *International Journal of Biological Macromolecules*, *44*(4), 372–378.
- Sasaki, T., & Noda, H. (1974). Studies on silk fibroin of Bombyx mori directly extracted from the silk gland: III. n-terminal analysis and degradation in a slightly alkaline solution. *Journal of Biochemistry*, *76*(3), 493–502.
- Ström, A., Larsson, A., & Okay, O. (2015). Preparation and physical properties of hyaluronic acid-based cryogels. *Journal of Applied Polymer Science*, *132*(29), 42194.
- Tavsanli, B., & Okay, O. (2016). Preparation and fracture process of high strength hyaluronic acid hydrogels cross-linked by ethylene glycol diglycidyl ether. *Reactive & Functional Polymers*, *109*, 42–51.
- Tavsanli, B., & Okay, O. (2017). Mechanically strong hyaluronic acid hydrogels with an interpenetrating network structure. *European Polymer Journal*, *94*, 185–195.
- Tavsanli, B., Can, V., & Okay, O. (2015). Mechanically strong triple network hydrogels based on hyaluronan and poly(N,N-dimethylacrylamide). *Soft Matter*, *11*(43), 8517–8524.
- Treloar, L. R. G. (1975). *The physics of rubber elasticity* (3rd ed.). USA: Oxford University Press.
- Uemura, Y., McNulty, J., & Macdonald, P. M. (1995). Associative behavior and diffusion coefficients of hydrophobically modified poly(N,N-dimethylacrylamides). *Macromolecules*, *28*(12), 4150–4158.
- Uzumcu, A. T., Guney, O., & Okay, O. (2018). Highly stretchable DNA/clay hydrogels with self-healing ability. *ACS Applied Materials & Interfaces*, *10*, 8296–8306.
- Valachova, K., Topolska, D., Mendichi, R., Collins, M. N., Sasinkova, V., & Soltes, L. (2016). Hydrogen peroxide generation by the Weissberger biogenic oxidative system during hyaluronan degradation. *Carbohydrate Polymers*, *148*, 189–193.
- Vepari, C., & Kaplan, D. L. (2007). Silk as a biomaterial. *Progress in Polymer Science*, *32*, 991–1007.
- Vollrath, F., & Porter, D. (2009). Silks as ancient models for modern polymers. *Polymer*, *50*, 5623–5632.
- Weng, L., Gouldstone, A., Wu, Y., & Chen, W. (2008). Mechanically strong double network photocrosslinked hydrogels from N,N-dimethylacrylamide and glycidyl methacrylated hyaluronan. *Biomaterials*, *29*(14), 2153–2163.
- Yan, S., Wang, Q., Tariq, Z., You, R., Li, X., Li, M., & Zhang, Q. (2018). Facile preparation of bioactive silk fibroin/hyaluronic acid hydrogels. *International Journal of Biological Macromolecules*, *118*, 775–782.
- Yang, X., Wang, X., Yu, F., Ma, L., Pan, X., Luo, G., & Wang, H. (2016). Hyaluronic acid/EDC/NHS-crosslinked green electrospun silk fibroin nanofibrous scaffolds for tissue engineering. *RSC Advances*, *6*(102), 99720–99728.
- Zamboni, F., Viera, S., Reis, R. L., Oliveira, J. M., & Collins, M. N. (2018). The potential of hyaluronic acid in immunoprotection and immunomodulation: Chemistry, processing and function. *Progress in Materials Science*, *97*, 97–122.
- Zhou, C.-Z. (2000). Fine organization of Bombyx mori fibroin heavy chain gene. *Nucleic Acids Research*, *28*(12), 2413–2419.
- Zhou, J., Zhang, B., Liu, X., Shi, L., Zhu, J., Wei, D., & He, D. (2016). Facile method to prepare silk fibroin/hyaluronic acid films for vascular endothelial growth factor release. *Carbohydrate Polymers*, *143*, 301–309.